Mueller polarimetry as a tool for detecting asymmetry in diffraction grating profiles

Tatiana Novikova[a] and Pavel Bulkin
LPICM, CNRS, Ecole Polytechnique, Palaiseau 91128, France

Vladimir Popov[b]
Skobeltsyn Institute of Nuclear Physics, Moscow State University, Russia

Bicher Haj Ibrahim and Antonello De Martino
LPICM, CNRS, Ecole Polytechnique, Palaiseau 91128, France

(Received 19 March 2011; accepted 19 July 2011; published 9 September 2011)

Reflected Mueller matrix spectra were measured and simulated for asymmetrical photoresist master diffraction gratings in conical mounting (i.e., the direction of grating grooves was not perpendicular to the plane of light incidence). From the electromagnetic reciprocity theorem, Mueller matrix of symmetric grating (composed of only reciprocal materials, and operating in zeroth-order diffraction) is invariant under transposition ($\boldsymbol{M} = \boldsymbol{M}^t$). For zeroth-order diffraction of asymmetric gratings, the lack of profile rotational symmetry violates this reciprocity and, consequently, breaks the symmetry of the above-mentioned matrix. This property of the Mueller matrix of asymmetric gratings was experimentally observed and numerically modeled at all experimental illumination conditions with the exception of planar mounting (the direction of grating grooves was perpendicular to the plane of light incidence), where there is no cross-polarization effect for the gratings composed of isotropic materials. It was demonstrated that optical nonreciprocity of diffraction gratings can be used for unambiguous detection of grating profile asymmetry. In addition, choosing optimal measurement configuration (i.e., azimuthal angles) considerably increases the sensitivity of the detection technique. © *2011 American Vacuum Society*.
[DOI: 10.1116/1.3633693]

I. INTRODUCTION

The metrology of nanogratings is of great importance for many industrial applications. With ever-shrinking chip critical dimensions (CDs) it has become one of the leading factors defining process performance in microelectronics.[1] Nanogratings applications such as laser pulse compression in chirped pulse amplification systems, antireflection structures, and counterfeit protection labels require consistent fabrication of a specified grating design. The nanoimprint grating replication process is widely used for the production of security holograms. These holograms represent the diffractive structures, composed mainly of diffraction gratings of varied pitches, critical dimensions, and orientations with respect to each other. These structures possess unique diffractive optical properties which are difficult to imitate and, consequently, have high fidelity against counterfeiting. The fabrication process typically consists of two steps: (1) the designed structure is translated into a resist layer (spin-coated over a substrate) by optical or electron-beam lithography and subsequent etching (the resulting structure is called a master grating); (2) nickel electroplating and mechanical separation of the metal layer deposited on top of the master grating yield a Ni shim. Afterward, the shim is used for the replication of the original structure in a soft plastic layer by either stamping or by the roll-to-roll process. The metrology of Step 1 is of crucial importance to the process, as this step is the most expensive and time consuming part of the replicative nanoimprint grating fabrication. Atomic force microscopy (AFM) and scanning electron microscopy (SEM) characterization techniques, widely used now for metrological applications,[2–5] can provide images of either the sample surface or the cleaved sample. Although accepted as "golden standards" for grating metrology, these techniques have some drawbacks. They are relatively slow, sometimes sample-destructive, and deliver only local information about samples. During the last few years, there has been growing interest in optical techniques (e.g., reflectometry, ellipsometry, scatterometry, polarimetry) that provide quality control of such structures.[6–8] The interaction of polarized light with a sample changes the polarimetric properties of the reflected (transmitted) beam, depending on the light wavelength, configuration of the measurement (polar and azimuthal angles), and properties of the sample (e.g., refractive indices of sample materials and geometry of the grating). Unlike AFM and SEM, optical measurement techniques are fast and nondestructive, and spatial information is averaged over the spot of the probing beam (typically the diameter of the spot is a few tens of microns).

In terms of Stokes formalism, any sample, even a depolarizing one, can be described by its real 4×4 Mueller matrix.[9] The measurements of the Mueller matrix at an arbitrary orientation of the plane of light incidence with respect to the direction of the grooves of one-dimensional (1D) grating (so called conical mounting) have proved to be a powerful optical

[a]Electronic mail: tatiana.novikova@polytechnique.edu
[b]Present address: General Physics Department, Moscow State University, Russia.

technique for the metrological characterization of diffraction gratings. It has been shown in our previous work that the grating profile can be successfully reconstructed via appropriate optical modeling using full Mueller matrix measurements.[7] We have also demonstrated that this approach can be of particular interest in microelectronics technology for the detection of overlay errors,[10] which frequently result from alignment deficiencies in lithography. In some cases, the asymmetrical distortion of a grating profile can be induced by the etch process, or even be intentional, like in blazed gratings fabrication. For these applications, a technique that allows for fast, noncontact evaluation of the profile asymmetry may be of great value.

With a spectroscopic polarimeter, we studied the Mueller matrix spectra of the asymmetric master gratings in a photoresist on a chromium-covered glass substrate in the most general geometry of conical diffraction. At conical mounting, the break of symmetry for two off diagonal 2×2 blocks of the Mueller matrix was predicted for zeroth order diffraction of asymmetric gratings (because of violation of the electromagnetic reciprocity theorem).[11] We experimentally observed and measured the difference in those elements of the Mueller matrices for the asymmetric gratings. With numerical modeling, we have shown that for diffraction grating this property of Mueller matrix elements can be exploited to detect the asymmetry of grating profile. We demonstrate that the sensitivity of the polarimetric measurements depends on the choice of azimuthal angle.

This paper is organized as follows: after the introduction (Sec. I), we describe the experimental setup, the studied samples, and show the results (Sec. II). The next part (Sec. III) is devoted to the comparison of the modeling and the experiments. Then we discuss the results (Sec. IV) and, finally, end by summarizing our conclusions (Sec. V).

II. EXPERIMENTAL METHODS

A. Samples and Experimental Setup

A layer of polymethyl methacrylate (PMMA) was spin-coated onto a chromium-covered glass substrate (15 cm $\times$ 15 cm). The master gratings were formed in this layer with electron beam lithography and subsequent wet etching. The sample consisted of 14 metrological boxes (size 7 mm $\times$ 7 mm) containing diffraction gratings with a 1.6 μm pitch [see Fig. 1(a)]. The e-beam exposure dose along the grating period was intentionally varied in order to produce an asymmetrical grating profile after etching. The asymmetry of the gratings was confirmed by the AFM measurements. The three-dimensional AFM image and reconstructed grating profile are shown in Figs. 1(b) and 1(c). Optical polarimetric characterization of the sample was performed with a spectroscopic Mueller polarimeter MM16 (Horiba Jobin Yvon). The complete Mueller matrix spectra were acquired on the metrological boxes within the spectral range from 450 nm to 800 nm at the angle of incidence 70° and at varying azimuthal angles (0° to 360°). The size of the spot in our measurements was around 0.5 mm $\times$ 1.5 mm, so the signal was integrated over a few hundreds of grating periods. Hence, the assumption of the diffraction on the infinite periodic structure was justified and used in our further study.

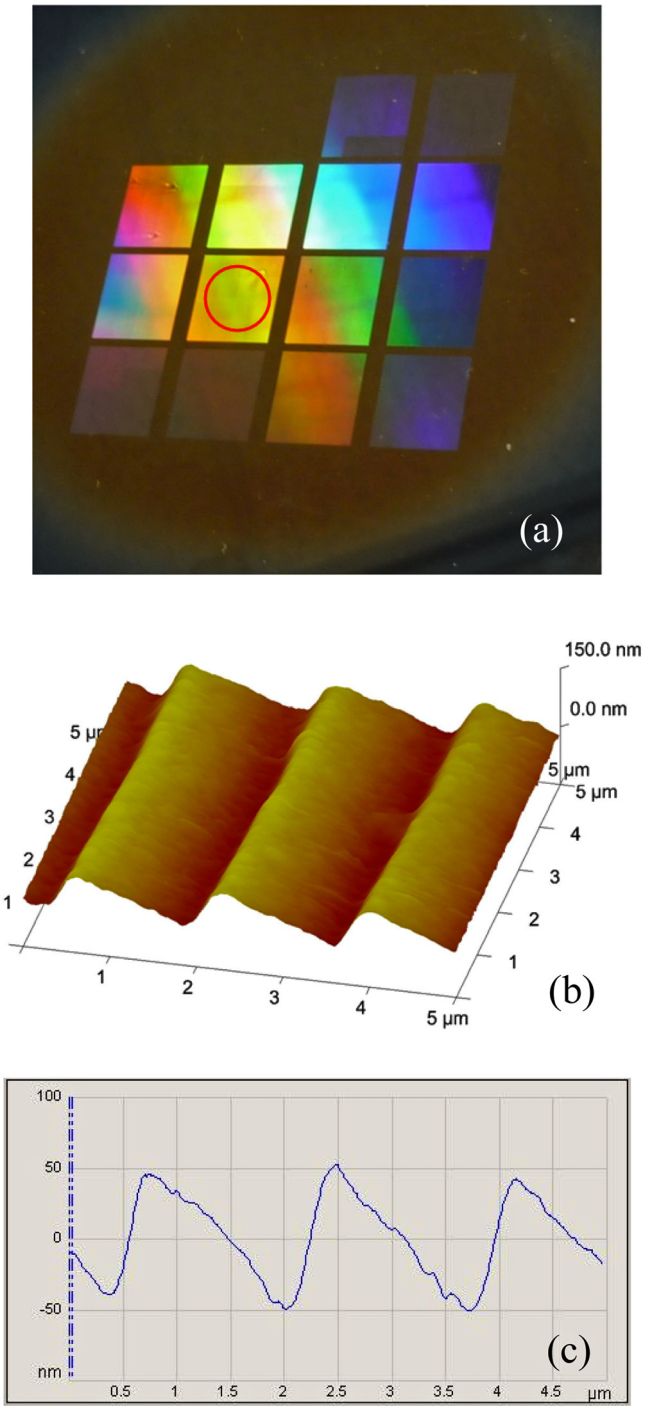

FIG. 1. (Color online) (a) Photo of resist master grating. The measured metrological box is shown with circle. (b) 3D reconstruction of AFM image of measured box. (c) Example of AFM profile of measured metrological box.

B. Theory and Measurements

For a given grating profile the following relation holds true for the elements of two 2×2 off diagonal blocks of the grating Mueller matrix because of mirror symmetry[12]:

$$m_{ij}(\varphi, \theta, \lambda) = -m_{ij}(-\varphi, \theta, \lambda), \quad (1)$$

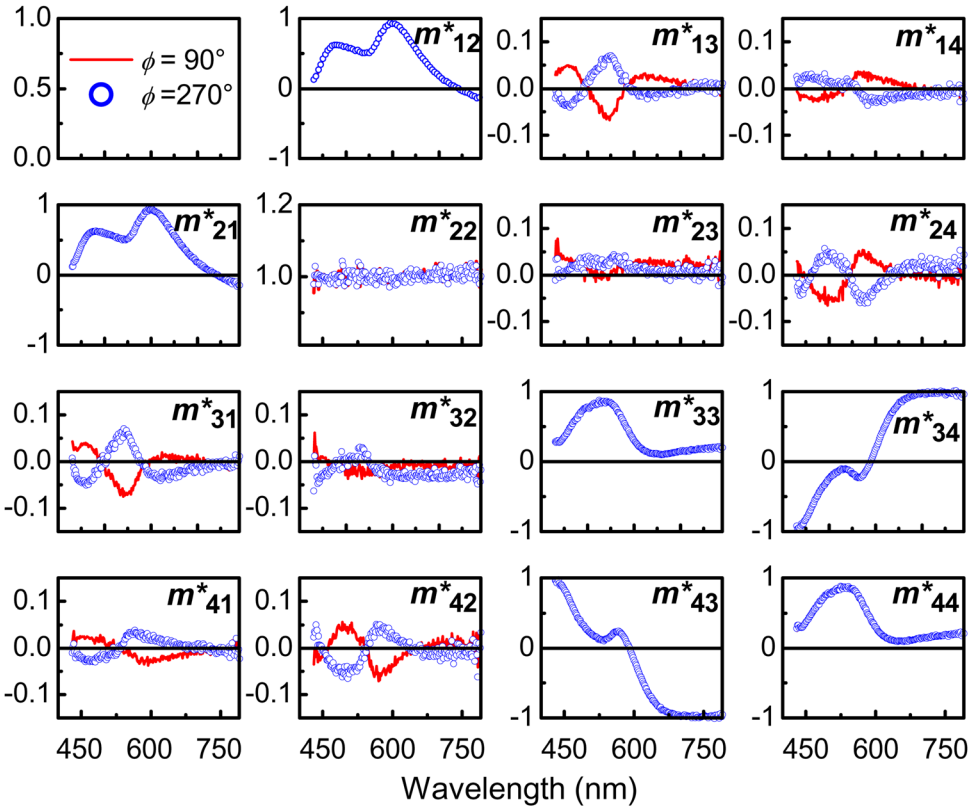

FIG. 2. (Color online) Measured complete Mueller matrix spectra at two reciprocal azimuthal angles $\phi = 90°$ (red line) and $\phi = 270°$ (blue open circles). All elements of Mueller matrices are normalized by m_{11} element, which is not shown here.

where ϕ is an azimuthal angle, θ is an angle of incidence, and λ is wavelength of the light.

It was shown by Li[11] that, at conical mounting, the zeroth order cross-polarization complex reflection coefficients of the grating are antisymmetric $[r^0_{sp}(\varphi,\theta,\lambda) = -r^0_{ps}(\varphi,\theta,\lambda)]$, provided that the grating is composed of only reciprocal materials and is invariant under the rotation by 180° about the normal incidence. This is a direct consequence of the electromagnetic reciprocity theorem for the zeroth diffracted order. It leads to the following relations between the elements of 2×2 off diagonal blocks of the Mueller matrix:

$$m_{13}(\varphi,\theta,\lambda) = -m_{31}(\varphi,\theta,\lambda) \quad m_{14}(\varphi,\theta,\lambda) = m_{41}(\varphi,\theta,\lambda)$$
$$m_{23}(\varphi,\theta,\lambda) = -m_{32}(\varphi,\theta,\lambda) \quad m_{24}(\varphi,\theta,\lambda) = m_{42}(\varphi,\theta,\lambda). \tag{2}$$

The asymmetry of the diffraction gratings violates the above-mentioned reciprocity. The absolute values of the transposed elements of 2×2 off diagonal blocks of the Mueller matrix in Eq. (1) change to: $|m_{ij}(\varphi,\theta,\lambda)| \neq |m_{ji}(\varphi,\theta,\lambda)|$. The pure conical mounting ($\varphi = \pm 90°$ or $\varphi = 90°, 270°$) is of particular interest, because as it follows from Eqs. (1) and (2), the elements of 2×2 off diagonal blocks of the Mueller matrix have to be equal to zero for a symmetric grating profile, while they can be different from zero for a asymmetric grating profile. The complete spectral Mueller matrices of the same metrological box measured at two reciprocal azimuthal configurations ($\varphi = 90°, 270°$) are plotted in Fig. 2. As shown, the elements of two off diagonal blocks are different from zero, as predicted by the theory for the asymmetric grating profile.

III. MODELING

The acquired spectral Mueller matrices of the gratings, measured at different azimuthal angles, are fitted with the parametric model of the grating profile shown in Fig. 3, where $H_{grating}$ is the height of the ridge, L is the top width (CD), and A and B are left and right slope projections of the trapezoid. While fitting the measured spectra, we noted overlap of the neighbor ridges. At that point, we introduced a continuous resist layer of thickness H_{layer} underneath the grating and consequently reduced the A and B values. This reflects the fact that the chromium surface was not open during the wet etching of the sample. The direct simulations of spectral Mueller matrices were performed with the rigorous coupled-wave analysis (RCWA) algorithm[13] and the S-matrix method.[14]

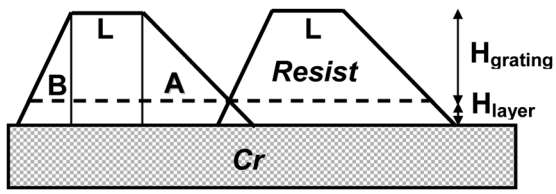

FIG. 3. Parametric model of grating profile.

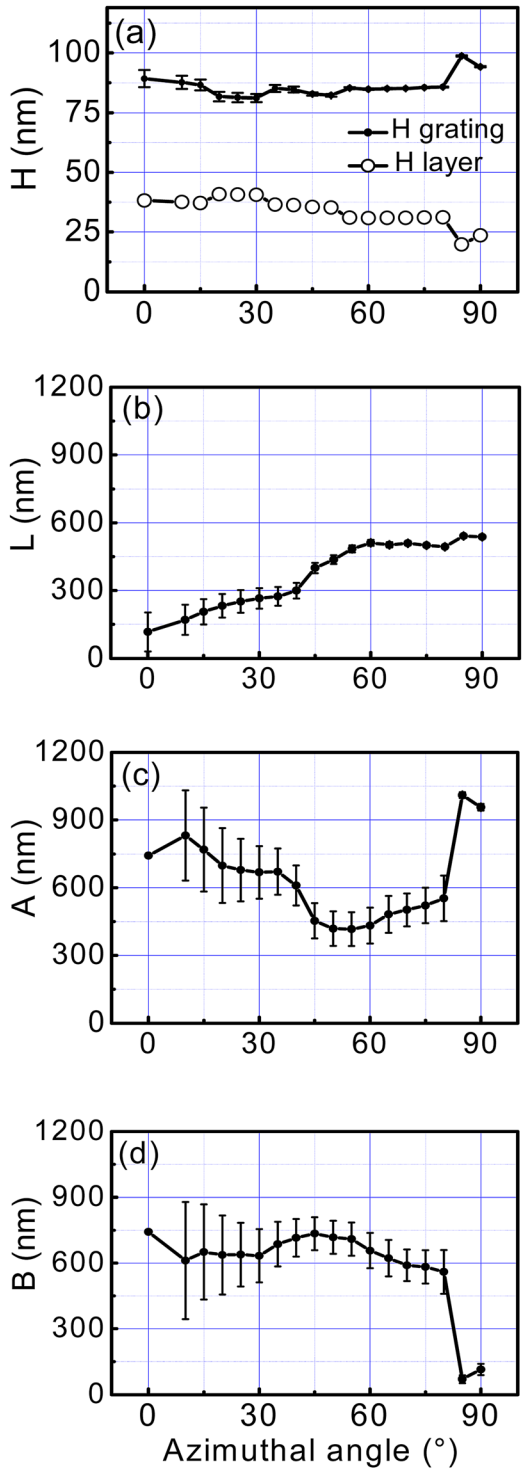

FIG. 4. (Color online) Optimal values of model parameters H, L, A, and B (see text) at different azimuthal angles.

Figure 4 shows the results of the fit for measurements at azimuthal angles from 0° to 90° at every 5° increment.

The standard uncertainties of the estimated parameter values were calculated as the square roots of the diagonal elements of the covariance matrix C_{ij}. This matrix is defined as the inverse of dispersion matrix $\alpha_{ij} = \sum_{k=1}^{N} 1/\sigma_k^2 \{[\partial m(p)_k/\partial p_i][\partial m(p)_k/\partial p_j]\}$, $i, j = 1,\ldots K$, where N is the number of measured spectral points, σ_k is the estimated uncertainty of the measurement, K is the number of floating parameters of the model ($K = 4$ in our case), p is the vector of model parameter values, and $\partial m(p)_k/\partial p_i$ is the derivative of Mueller matrix elements at the spectral point k with respect to model parameter p_i. We assume that the errors for the raw data are not statistically correlated and have the same standard deviations equal to the measurement accuracy (0.015).

The variance analysis shows that optimal values of parameters of the model (H, L, A, and B) have the smallest errors for the azimuthal angles φ closest to 90° (plane of light incidence is parallel to the grating grooves). The largest parameter errors are for the angles φ closest to 0° (plane of light incidence is perpendicular to the grating grooves). Moreover, for two parameters A and B, the errors are infinitely large at $\varphi = 0°$ [not shown in Fig. 4(c) and 4(d)] because of very high parameter correlation at this measurement configuration. Fitting the data acquired at different azimuthal angles (0°–80°) gives no direct evidence of the profile asymmetry [Fig. 4(c) and 4(d)]. The optimal values of parameters A and B look the same, given the parameters' errors. The measurements at azimuthal angles close to $\varphi = 90°$ reveal the strong asymmetry of the grating profile with relatively small parameter errors [see Fig. 4(c) and 4(d)].

To further study this effect, we repeated the measurements and the fit of experimental spectra, varying the azimuthal angle φ from 0° to 360° by increments of 15°. The parametric model of gratings was modified according to the results of the previous fit. The continuous layer of PMMA resist with a fixed thickness of 33 nm was added to the model (see Fig. 5).

IV. RESULTS AND DISCUSSION

A. Calculated optimal parameter values

The optimal values of model parameters versus different azimuthal angles are shown in Fig. 6. The optimal values of grating height H exhibit periodic behavior with the period of 90° with maximal values at $\varphi = 0°$, 90°, 180°, and 270° (planar and pure conical configurations) [Fig. 6 (a)]. The optimal values of L (top width of grating ridge) have two minima at $\varphi = 90°$ and 270°, and vary significantly at other azimuthal angles [Fig. 6 (b)]. The dependence of the optimal values of A and B on azimuthal angle is more complex. It should be noted that at pure conical mounting ($\varphi = 90°$ and 270°), parameter A dips to a minimum value, while parameter B reaches a maximum value. At the same time, the values of A and B are flipped at the angles close to planar diffraction ($\varphi = 0°$ and

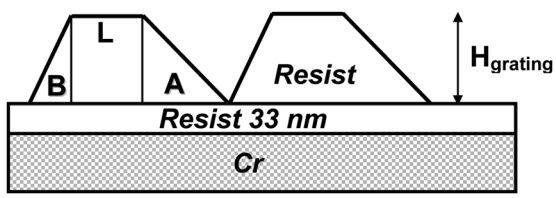

FIG. 5. Modified parametric model of the grating. The thickness of continuous resist layer under grating is fixed at 33 nm.

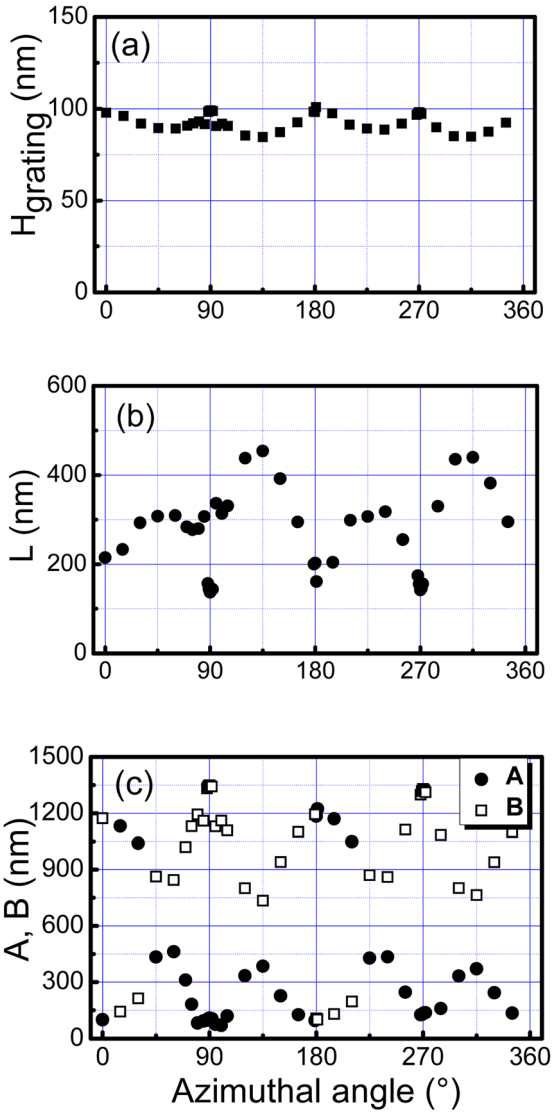

FIG. 6. (Color online) Optimal values of parameters H, L, A, and B of modified model at different azimuthal angles.

180°) [see Fig. 6(c)]. In order to understand qualitatively the flip of parameters A and B, we performed the following calculations. We fixed the optimal values of parameter H at 100 nm and parameter L at 150 nm while varying the values of A and B independently from 0 to 1500 nm. For each chosen set of parameters H, L, A, and B we calculated the merit function (mean square distance) according to Eq. (3),

$$D^2 = \frac{1}{N}\left[\sum_{k=1}^{N}\frac{1}{15}\sum_{ij}\left(m^k_{ij,\mathrm{exp}} * - m^k_{ij,\mathrm{sim}} *\right)^2\right], \tag{3}$$

where $m^k_{ij,\mathrm{exp}}* = m^k_{ij,\mathrm{exp}}/m^k_{11,\mathrm{exp}}$ and $m^k_{ij,\mathrm{sim}}* = m^k_{ij,\mathrm{sim}}/m^k_{11,\mathrm{sim}}$ (i, j =1,4, k = 1,..,N, where N is a number of spectral points) are the spectra of 15 normalized measured and simulated Mueller matrix coefficients at $\varphi = 0°$ and 90°.

B. Maps of merit function at different azimuths

The maps of D^2 values versus A and B values at two different azimuthal angles $\varphi = 0°$ and 90° are shown in Fig. 7.

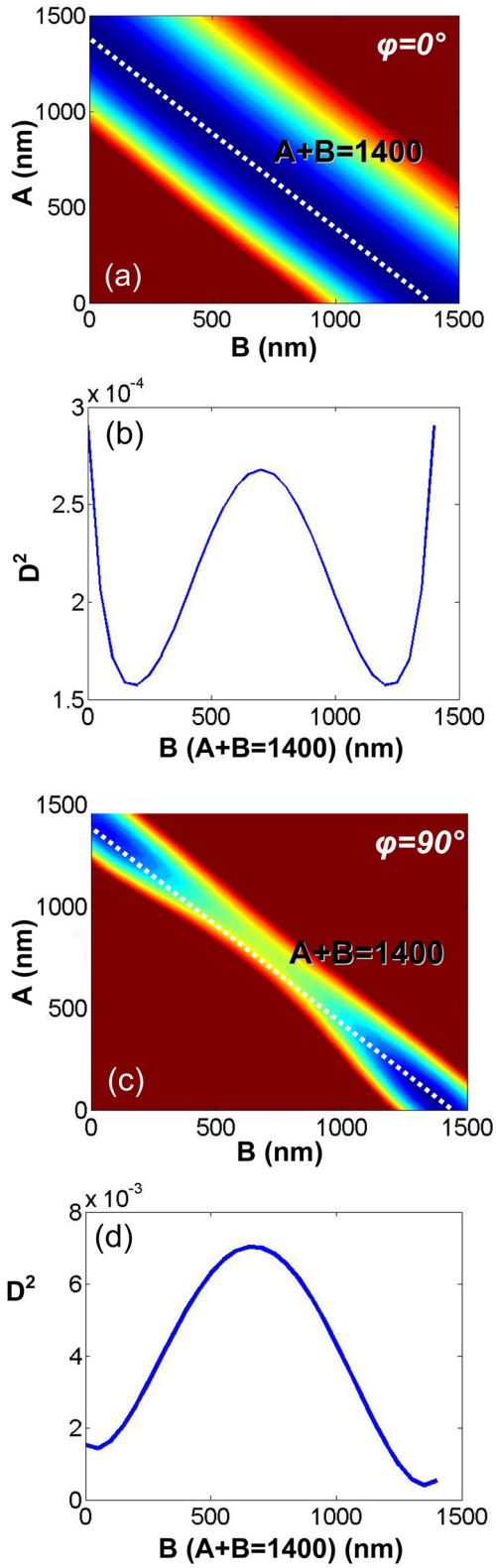

FIG. 7. (Color online) Maps of merit function D^2 at azimuthal angle (a) $\phi = 0°$, (b) profile extracted along the dotted line at $\phi = 0°$, (c) $\phi = 90°$, (d) profile extracted along the dotted line at $\phi = 90°$.

The dotted lines on Fig. 7(a) and 7(c) correspond to the values of A + B = 1400 nm. At $\varphi = 0°$, the surface of D^2 has a valley oriented along this line. The values of D^2 extracted along the dotted line are plotted in Fig. 7(b). It is clearly

shown that the merit function has two equivalent minima at the points A = 200 nm, B = 1200 nm and A = 1200 nm, B = 200 nm. In the planar configuration, the deviation of the profile from the symmetric one is visible, but it is impossible to distinguish between right- (A>B) or left- (A<B) sided trapezoids. Thus, the flip of A and B values at the measurement configurations close to the planar one can be easily induced by the measurement noise, which is always present. Depending on the initial guess, the fit procedure can converge to any of two existing minima of the merit function. Conversely, at conical mounting (φ= 90°) the valley of merit function transforms into asymmetric one along the dashed line [see Fig. 7(d)]. The data extracted along the same line A + B = 1400 nm then showed only one global minimum located at the point A = 50 nm, B = 1350 nm. At the angles φ close to 90° or 270° the fit procedure always converged to the same values of A and B (A < B). The asymmetry of the profile found from the fit of spectral Mueller matrix coefficients is consistent with AFM measurements of the sample. At conical mounting, not only the distortion of the symmetric profile can be detected, but the direction of the displacement can be identified.

V. SUMMARY AND CONCLUSIONS

The metrological studies of asymmetric resist gratings with the pitch of 1.6 μm on chromium-covered glass substrate, used for the fabrication of the master grating in the nanoimprint fabrication process, were performed with a spectroscopic Mueller polarimeter at a fixed angle of incidence 70° and varied azimuthal angles (0°<φ <360°). The acquired spectra were fitted with the asymmetric trapezoid model. From the variance analysis, the smallest parameter errors are found at the azimuthal angles close to pure conical mounting (φ = 90° ± 10° or 270° ± 10°). Compared to planar configuration (φ = 0° or 180°), these results are robust and less sensitive to the measurement noise. We propose that grating profile symmetry check should be performed using polarimetric measurement at azimuthal angles close to conical mounting, and not those close to planar mounting. It was experimentally observed and numerically modeled that not only the distortion of the symmetric profile can be detected but the direction of the displacement (left or right) can also be identified provided the Mueller matrix of grating is measured at conical mounting. This property of Mueller matrices could be exploited for the unambiguous characterization of the asymmetry in grating profiles.

ACKNOWLEDGMENT

Funding from Agence nationale de la recherche (ANR) through the project MuellerFourier is gratefully acknowledged.

[1]See: International Technology Roadmap for Semiconductors, http://www.itrs.net/.
[2]R. G. Dixson, R. A. Allen, W. F. Guthrie, and M. W. Cresswell, J. Vac. Sci. Technol. B **23**, 3028 (2005).
[3]N. G. Orji, T. V. Vorburger, J. Fu, R. G. Dixson, C. V. Nguyen, and J. Raja, Meas. Sci. Technol. **16**, 2147 (2005).
[4]J. J. Hwu. S. Babin, and K. Bay, Proc. SPIE **7638**, 76383O (2010).
[5]V. A. Ukraintsev and J. Foucher, Proc. SPIE **7638**, 76381C (2010).
[6]R. Alassaad, S. Regonda, L. Tao, S. Pang, and W. Hu, J. Vacuum Sci. Technol. B **25**, 2396 (2007).
[7]T. Novikova, A. De Martino, S. Ben Hatit, and B. Drévillon, Appl. Opt. **45**, 3688 (2006).
[8]T. Novikova, A. De Martino, P. Bulkin, Q. Nguyen, B. Drévillon, V. Popov, and A. Chumakov, Opt. Express **15**, 2033 (2007).
[9]D. Goldstein, *Polarized Light*, 2nd ed. (Marcel Dekker, New York, 2003).
[10]T. Novikova, A. De Martino, R. Ossikovski, and B. Drévillon, Eur. Phys. J. Appl. Phys. **31**, 63 (2005).
[11]L. Li, Opt. Soc. Am. A **17**, 881 (2000).
[12]S. Ben Hatit, M. Foldyna, A. De Martino, and B. Drévillon, Phys. Status Solidi A **4**, 743 (2008).
[13]M. G. Moharam, E. B. Grann, D. A. Pommet, and T. K. Gaylord, J. Opt. Soc. Am. A **12**, 1068 (1995).
[14]L. Li, J. Opt. Soc. Am. A **13**, 1024 (1996).